Chemistry of Phosphido-Bridged Mixed-Metal Complexes. Insertion of Alkynes into the Phosphido Bridge of $(CO)_4Ru(\mu\text{-}PPh_2)Co(CO)_3$. X-ray Structures of $(CO)_3Ru(\mu\text{-}Ph_2PC(O)C(Ph)=C(Ph))Co(CO)_3$, $(CO)_3Ru(\mu\text{-}Ph_2PC(O)C(SiMe_3)=C(H))Co(CO)_3$, and $(CO)_3Ru(\mu\text{-}Ph_2PC(Ph)=C(Ph))Co(CO)_3$

Rachid Regragui and Pierre H. Dixneuf*

Laboratoire de Chimie de Coordination Organique, URA CNRS D0415, Campus de Beaulieu, Université de Rennes, 35042 Rennes Cedex, France

Nicholas J. Taylor and Arthur J. Carty*

Guelph-Waterloo Centre for Graduate Work in Chemistry, Waterloo Campus, Department of Chemistry, University of Waterloo, Waterloo, Ontario, Canada N2L 3G1

Received November 30, 1989

The synthesis and characterization of two series of heterobinuclear Ru–Co complexes are described: $(OC)_3Ru(\mu\text{-}\eta^3\text{-}Ph_2PCOC(R^1)=C(R^2))Co(CO)_3$ (**2**; R^1, R^2 = Ph, Ph (**a**), Ph, C≡CPh (**b**), H, Ph (**c**), H, ^{t}Bu (**d**), $SiMe_3$, H (**e**), H, H (**f**)) and $(OC)_3Ru(\mu\text{-}\eta^3\text{-}Ph_2PC(R^1)=C(R^2))Co(CO)_3$ (**3a–d**). Complexes **2** result from the regioselective reaction at 30–35 °C of alkynes **a–f** with $(OC)_4Ru(\mu\text{-}PPh_2)Co(CO)_3$ **1**, which has a very reactive phosphido bridge. Decarbonylation of complexes **2a–d** at 60–65 °C affords complexes **3a–d**. The reversibility of the insertion of the alkyne in **2a** is shown by its reaction with ^{t}BuC≡CH, which leads to **2d**. Complexes **2a**, **2c**, and **2e** react with Ph_2PH to give the carbonyl monosubstitution products $(Ph_2PH)(CO)_2Ru(Ph_2PCOC(R^1)=C(R^2))Co(CO)_3$ (**4**). Molecular structures of **2a**, **2e**, and **3a** have been determined by X-ray diffraction. Crystal data: **2a**, triclinic, space group $P\bar{1}$, a = 8.280 (1) Å, b = 12.419 (2) Å, c = 14.966 (2) Å, α = 99.58 (1)°, β = 99.55 (1)°, γ = 90.10 (1)°, Z = 2; **2e**, monoclinic, space group $I2/a$, a = 17.054 (2) Å, b = 10.846 (2) Å, c = 30.671 (4) Å, β = 107.81 (1)°, Z = 8; **3a**, monoclinic, space group $P2_1/c$, a = 17.041 (2) Å, b = 10.721 (1) Å, c = 17.511 (2) Å, β = 101.56 (1)°, Z = 4. Each structure shows a bonding Ru–Co interaction (**2a**, 2.6577 (4) Å; **2e**, 2.6710 (6) Å; **3a**, 2.6479 (7) Å), Ru–C(R^2) and Ru–P linkages, and the presence of a five-membered (**2a**, **2e**) or four-membered metallacycle (**3a**) with coordination of the C(R^1)=C(R^2) double bond to the cobalt atom.

Introduction

The participation of phosphido groups in the chemistry of bi- and polynuclear μ-PR_2 complexes is now well established,[1] and insertion of small molecules into M–(μ-PR_2)–M systems has provided routes to some novel bridging ligands, including the general class μ-R_2P=X (X = O,[2] X = CH_2 or CRR'[3,4]), alkenyl- and butadienylphosphines,[5] and diphosphines.[6] We have been exploring in detail the chemistry of the binuclear μ-PPh_2 mixed-metal complex $(OC)_4Ru(\mu\text{-}PPh_2)Co(CO)_3$ (**1**),[7-11] and in a preliminary communication we described the insertion of diphenylacetylene and CO into the phosphido bridge, affording (alkenylcarbonyl)phosphine and alkenylphosphine ligands.[10] Although examples of P–C coupling reactions involving phosphido groups and acetylenes have been rare until recently,[12-14] there has been an increasing number of reports of alkyne insertions into both μ-PR_2 and μ-PR bridges.[15-18] Such reactions have potential for the generation of new P–C bonds and for the introduction of carbon fragments into clusters. In this paper we describe in detail the reactions of **1** with mono- and disubstituted acetylenes $R^1C{\equiv}CR^2$ to generate the complexes $RuCo(CO)_6(\mu\text{-}PPh_2C(O)C(R^1)=C(R^2))$ (**2**) and their decarbonylation products $RuCo(CO)_6(\mu\text{-}PPh_2C(R^1)=C(R^2))$ (**3**),

(1) For a selection of recent references to phosphido bridge reactivity see: (a) Rosenberg, S.; Geoffroy, G. L.; Rheingold, A. L. *Organometallics* **1985**, *4*, 1184. (b) Nucciarone, D.; MacLaughlin, S. A.; Taylor, N. J.; Carty, A. J. *Organometallics* **1988**, *7*, 106.

(2) Klingert, B.; Werner, H. *J. Organomet. Chem.* **1983**, *252*, C47.

(3) (a) Yu, Y. F.; Chan, C. N.; Wojcicki, A.; Calligaris, M.; Nardin, G.; Balducci, G. *J. Am. Chem. Soc.* **1984**, *106*, 3704. (b) Yu, Y. F.; Galluci, J.; Wojcicki, A. *J. Chem. Soc., Chem. Commun.* **1984**, 653. (c) Rosenberg, S.; Whittle, R. R.; Geoffroy, G. L. *J. Am. Chem. Soc.* **1984**, *106*, 5934. (d) Rosenberg, S.; Geoffroy, G. L.; Rheingold, A. L. *Organometallics* **1985**, *4*, 1184.

(4) (a) Werner, H.; Zolk, R. *Organometallics* **1985**, *4*, 601. (b) Werner, H.; Zolk, R. *Chem. Ber.* **1987**, *120*, 1003.

(5) (a) Henrich, K.; Iggo, J. A.; Mays, M. J.; Raithby, P. R. *J. Chem. Soc., Chem. Commun.* **1984**, 209. (b) Henrick, K.; McPartlin, M.; Iggo, J. A.; Kemball, A. C.; Mays, M. J.; Raithby, P. R. *J. Chem. Soc., Dalton Trans.* **1981**, 2669. (c) Horton, A. D.; Mays, M. J.; Raithby, P. R. *J. Chem. Soc., Chem. Commun.* **1985**, 247.

(6) (a) Yu, Y. F.; Chan, C. N.; Wojcicki, A.; Calligaris, M.; Nardin, G.; Balducci, G. *J. Am. Chem. Soc.* **1984**, *106*, 3104. (b) Yu, Y. F.; Wojcicki, A.; Calligaris, M.; Nardin, G. *Organometallics* **1986**, *5*, 47.

(7) (a) Regragui, R.; Dixneuf, P. H. *J. Organomet. Chem.* **1982**, *239*, C12. (b) Regragui, R.; Dixneuf, P. H.; Taylor, N. J.; Carty, A. J. *Organometallics* **1984**, *3*, 1020.

(8) Regragui, R.; Dixneuf, P. H.; Taylor, N. J.; Carty, A. J. *Organometallics* **1986**, *5*, 1.

(9) (a) Guesmi, S.; Dixneuf, P. H.; Taylor, N. J.; Carty, A. J. *J. Organomet. Chem.* **1986**, *303*, C47. (b) Guesmi, S.; Dixneuf, P. H.; Süss-Fink, G.; Taylor, N. J.; Carty, A. J. *Organometallics* **1989**, *8*, 307. (c) Guesmi, S.; Taylor, N. J.; Dixneuf, P. H.; Carty, A. J. *Organometallics* **1986**, *5*, 1964.

(10) Regragui, R.; Dixneuf, P. H.; Taylor, N. J.; Carty, A. J. *Organometallics* **1984**, *3*, 814.

(11) (a) Regragui, R.; Dixneuf, P. H. *J. Organomet. Chem.* **1988**, *344*, C11. (b) Regragui, R.; Dixneuf, P. H. *New J. Chem.* **1988**, *12*, 547.

(12) (a) Yasufuku, K.; Yamazaki, H. *J. Organomet. Chem.* **1972**, *35*, 367. (b) Bamett, B.; Krüger, C. *Cryst. Struct. Commun.* **1973**, *2*, 347.

(13) Smith, W. F.; Taylor, N. J.; Carty, A. J. *J. Chem. Soc., Chem. Commun.* **1976**, 896.

(14) Carty, A. J. *Adv. Chem. Ser.* **1982**, *No. 196*, 163.

(15) Zolk, R.; Werner, H. *J. Organomet. Chem.* **1983**, *252*, C53.

(16) Knoll, K.; Orama, A.; Huttner, G. *Angew. Chem., Int. Ed. Engl.* **1984**, *23*, 976.

(17) Lunniss, J.; MacLaughlin, S. A.; Carty, A. J.; Sappa, E. *Organometallics* **1985**, *4*, 2066.

(18) For a recent review of reactions of alkynes with phosphinidene clusters see: Knoll, K.; Huttner, G. *Angew. Chem., Int. Ed. Engl.* **1987**, *26*, 743.

0276-7333/90/2309-2234$02.50/0

the exchange of alkynes in **2**, and the X-ray structures of **2a** ($R^1 = R^2 = Ph$), **2e** ($R^1 = SiMe_3$, $R^2 = H$), and **3a** ($R^1 = R^2 = Ph$).

Experimental Section

General Procedures. Standard techniques, with Schlenk type equipment for the manipulation of air-sensitive compounds under a blanket of nitrogen, were employed. All solvents were dried (sodium benzophenone ketyl for THF and ether, CaH_2 for hexane and benzene, and P_2O_5 for CH_2Cl_2) and nitrogen-saturated prior to use. Chromatographic separations were made on thick-layer plates of Merck silica gel.

Instrumentation. Infrared spectra were recorded on Perkin-Elmer 225 and 457 instruments using either Nujol mulls or cyclohexane solutions in matched 0.5-mm NaCl cells. ^1H and ^{31}P NMR spectra were generally measured on a Bruker WP-80 spectrometer operating at 80 MHz for ^1H, 32.38 MHz for ^{31}P, and 20.115 MHz for ^{13}C or on a Bruker AC 300 spectrometer operating at 300.13 MHz for ^1H. ^{31}P spectra were proton noise decoupled, and shifts are reported relative to external 85% H_3PO_4. ^1H and ^{13}C shifts are relative to Me_4Si. Microanalyses were obtained from the CNRS laboratory, Villeurbanne, France.

Syntheses. Synthesis of $(CO)_3Ru(\mu\text{-}Ph_2PC(O)C(R^1)=C(R^2))Co(CO)_3$ (2). Complex 1[7] (1 mmol, 0.54 g) and 1 mmol of an alkyne were dissolved in 60 mL of THF. The orange mixture was stirred at 30–35 °C and became progressively red. The reaction was monitored by infrared spectra of cyclohexane solutions and by thin-layer chromatography on silica gel plates (eluant hexane). The residual orange complex **1** migrates first, followed by a small amount of the orange derivative **3** and then by the yellow-orange major product **2**. After 12 h at 30–35 °C the solvent was removed under vacuum. The products were dissolved in 2–3 mL of dichloromethane and chromatographed on a column of Florisil. To eliminate residual complexes **1** and **3** from **2**, hexane was used as the eluant and then a dichloromethane–hexane mixture eluted complex **2**, which was recrystallized from a dichloromethane–ether mixture.

Complex 2a was obtained from 0.18 g (1 mmol) of diphenylacetylene in 80% (0.58 g) yield; mp 168–170 °C. Anal. Calcd for $C_{33}H_{20}O_7PCoRu$: C, 55.10; H, 2.80; P, 4.30. Found: C, 55.21; H, 2.74; P, 4.40. MS: m/e 664 ($[M - 2CO]^+$), 636 ($[M - 3CO]^+$), 608 ($[M - 4CO]^+$), 580 ($[M - 5CO]^+$), 552 ($[M - 6CO]^+$), 523.966 (calcd for $[M - 7CO]^+$ ($C_{26}H_{20}PCo^{102}Ru$) 523.968). In addition ions corresponding to the formation of **1** (m/e 542 ($M_1^+ = [RuCo(CO)_7(PPh_2)]^+$), 513.860 (calcd for $[M - CO]^+$ ($C_{18}H_{10}O_6PCo^{102}Ru$) 513.859)) were observed. IR (C_6H_{12}, ν_{CO}, cm^{-1}): 2093 (m), 2039 (s), 2022 (m), 1994 (m), 1878 (w) 1608 (vs). $^{31}P\{^1H\}$ NMR (32.38 MHz, CD_2Cl_2, 300 K, δ (ppm)): +38.6. ^1H NMR (80.00 MHz, CD_2Cl_2, 300 K, δ (ppm)): 7.45 (m, C_6H_5).

Complex 2b was obtained from 0.20 g (1 mmol) of 1,4-diphenylbutadiyne in 70% (0.52 g) yield; mp 160–165 °C. IR (C_6H_{12}, ν_{CO}, cm^{-1}): 2130 (vs), 2096 (m), 2042 (s), 2022 (m), 2007 (m), 1898 (w), 1611 (vs). $^{31}P\{^1H\}$ NMR (32.38 MHz, CD_2Cl_2, 300 K, δ (ppm)): +39.4. ^1H NMR (80.00 MHz, CD_2Cl_2, 300 K, δ (ppm)): 7.43 (m, C_6H_5).

Complex 2c was obtained from 0.10 g (1 mmol) of phenylacetylene in 80% (0.50 g) yield; mp 163–165 °C. IR (C_6H_{12}, ν_{CO}, cm^{-1}): 2094 (m), 2045 (s), 2025 (m), 2008 (m), 1900 (w), 1606 (vs). $^{31}P\{^1H\}$ NMR (32.38 MHz, CD_2Cl_2, 300 K, δ (ppm)): 42.9. ^1H NMR (80.00 MHz, CD_2Cl_2, 300 K, δ (ppm)): 7.44 (m, C_6H_5); 5.43 (d, $^3J_{PH}$ = 38 Hz, P–CO–C*H*=).

Complex 2d was obtained from 0.08 g (1 mmol) of 3,3-dimethylbutyne in 70% (0.44 g) yield; mp 172–175 °C. IR (C_6H_{12}, ν_{CO}, cm^{-1}): 2096 (m), 2045 (s), 2022 (m), 2008 (m), 1897 (w), 1610 (vs). $^{31}P\{^1H\}$ NMR (32.38 MHz, CD_2Cl_2, 300 K, δ (ppm)): +42.9. ^1H NMR (80.00 MHz, CD_2Cl_2, 300 K, δ (ppm)): 7.45 (m, C_6H_5); 5.44 (d, $^3J_{PH}$ = 38 Hz, P–CO–C*H*=); 1.27 (s, ^{t}Bu).

Complex 2e was obtained from 0.10 g (1 mmol) of (trimethylsilyl)acetylene in 85% (0.54 g) yield. The same yield was obtained when the mixture was heated for 6 h at 65 °C instead of 12 h at 30–35 °C; mp 190–200 °C dec. Anal. Calcd for $C_{24}H_{20}O_7PSiCoRu$: C, 45.08; H, 3.15; P, 4.84; Si, 4.39. Found: C, 45.44; H, 3.17; P, 4.82; Si, 3.87. IR (C_6H_{12}, ν_{CO}, cm^{-1}): 2090 (m), 2035 (s), 2018 (m), 1994 (m), 1893 (m, broad), 1602 (w). $^{31}P\{^1H\}$ NMR (32.38 MHz, $CDCl_3$, 300 K, δ (ppm)): +50.50. ^1H NMR (300.13 MHz, $CDCl_3$, 300 K, δ (ppm)): 8.65 (d, Ru–CH=, $^2J_{PH}$ = 1.3 Hz); 7.95–7.20 (m, C_6H_5); 0.26 (s, $SiMe_3$).

Complex 2f was obtained by reaction of 1 mmol of **1** in 60 mL of THF with an excess of acetylene (1 atm) for 7 days at room temperature. Red crystals were obtained in 90% (0.51 g) yield; mp 165–170 °C dec. Anal. Calcd for $C_{21}H_{12}O_7PCoRu$: C, 44.46; H, 2.13; P, 5.46. Found: C, 44.52; H, 2.15; P, 5.44. IR (C_6H_{12}, ν_{CO}, cm^{-1}): 2092 (m), 2036 (s), 2018 (m), 2000 (m), 1900 (w), 1625 (w). $^{31}P\{^1H\}$ NMR (32.38 MHz, $CDCl_3$, 300 K, δ (ppm)): +37.40 (s). ^{31}P NMR (δ (ppm)): +37.40 (d, $^3J_{PH}$ = 39.6 Hz). ^1H NMR (300.13 MHz, $CDCl_3$, 300 K, δ (ppm)): 8.19 (dd, Ru–CH=, $^3J_{HH}$ = 6.6 Hz, $^2J_{PH}$ = 1.1 Hz); 7.95–7.25 (m, C_6H_5); 5.43 (dd, =CH–CO–, $^3J_{HH}$ = 6.6 Hz, $^3J_{PH}$ = 38.00 Hz).

Synthesis of $(OC)_3Ru(\mu\text{-}\eta^3\text{-}Ph_2PC(R^1)=C(R^2))Co(CO)_3$ (3). Method A from Complex 1. Complex 1[7] (1 mmol, 0.54 g) and 1 mmol of an alkyne were dissolved in 60 mL of THF, and the mixture was stirred at 60–65 °C for 6 h. The solvent was evaporated, and the products were dissolved in 2–3 mL of dichloromethane and chromatographed on a column of Florisil (eluant hexane). A first red fraction contained the residual complex **1**, and then complex **3** was eluted. Complexes **3** were recrystallized from hexane.

Method B from Complexes 2. Complex **2** (0.5 mmol) was dissolved in 40 mL of THF, and the mixture was heated for 6 h at 60–65 °C. The reaction products were chromatographed on a column of Florisil (eluant hexane), and the orange isolated complex **3** was recrystallized from hexane.

Complex 3a ($R^1 = R^2 = Ph$). Method A. From 0.54 g of **1** and 0.18 g of diphenylacetylene, 0.40 g (60%) of yellow-orange crystals of **3a** was obtained.

Method B. From 0.36 g (0.5 mmol) of **2a**, 0.19 g (55%) of **3a** was obtained; mp 180–182 °C. Anal. Calcd for $C_{32}H_{20}O_6PCoRu$: C, 55.58; H, 2.91; P, 4.48. Found: C, 55.38; H, 2.94; P, 4.19. MS: m/e 692 ($[M]^+$), 663.945 (calcd for $[M - CO]^+$ ($C_{31}H_{20}O_5PCo^{102}Ru$) 663.942), 636 ($[M - 2CO]^+$), 608 ($[M - 3CO]^+$), 580 ($[M - 4CO]^+$), 552 ($[M - 5CO]^+$), 524 ($[M - 6CO]^+$), 496 ($[M - 7CO]^+$). Ions corresponding to the decomposition products of complexes **3** were also found: $Ru_2(\mu\text{-}PPh_2)_2(CO)_6$, m/e 742 ($[M]^+$), 713.884 (calcd for $[M - CO]^+$ ($C_{29}H_{20}O_5P_2Ru_2$) 713.887). IR (C_6H_{12}, ν_{CO}, cm^{-1}): 2080 (m), 2027 (s), 2021 (m), 2007 (w), 1984 (m), 1897 (w). $^{31}P\{^1H\}$ NMR (32.38 MHz, CD_2Cl_2, 300 K, δ (ppm)): –28.6. ^1H NMR (80.00 MHz, CD_2Cl_2, 300 K, δ (ppm)): 7.42 (m, C_6H_5).

Complex 3b (R^1 = Ph; R^2 = –C≡CPh). Method A. From 0.54 g of **1** and 0.2 g (1 mmol) of 1,4-diphenylbutadiyne, 0.46 g (65%) of **3b** was obtained.

Method B. From 0.37 g (0.5 mmol) of **2b**, 0.21 g (60%) of **3b** was obtained; mp 170–175 °C. IR (C_6H_{12}, ν_{CO}, cm^{-1}): 2079 (m), 2033 (s), 2021 (m), 2006 (m), 1993 (m), 1908 (vs). $^{31}P\{^1H\}$ NMR (32.38 MHz, CD_2Cl_2, 300 K, δ (ppm)): –21.7. ^1H NMR (80.00 MHz, CD_2Cl_2, 300 K, δ (ppm)): 7.43 (m, C_6H_5).

Complex 3c (R^1 = H, R^2 = Ph). Method A. From 0.54 g of **1** and 0.10 g of phenylacetylene, 0.40 g (65%) of red-brown crystals of **3c** was obtained.

Method B. From 0.33 g (0.5 mmol) of **2c**, 0.20 g (60%) of **3c** was obtained; mp 178–185 °C. IR (C_6H_{12}, ν_{CO}, cm^{-1}): 2078 (m), 2029 (s), 2018 (m), 1994 (ws), 1980 (m), 1890 (vs). $^{31}P\{^1H\}$ NMR (32.38 MHz, CD_2Cl_2, 300 K, δ (ppm)): –30.6 (s). ^1H NMR (80.00 MHz, CD_2Cl_2, 300 K, δ (ppm)): 7.42 (m, C_6H_5); 5.10 (d, P–CH=, $^2J_{PH}$ = 6.0 Hz).

Complex 3d (R^1 = H, R^2 = ^{t}Bu). Method A. From 0.54 g of **1** and 0.08 g (1 mmol) of 3,3-dimethylbutyne, 0.36 g (60%) of dark red crystals was obtained.

Method B. From 0.31 g (0.5 mmol) of **2d**, 0.15 g (50%) of **3d** was obtained; mp 185–190 °C. IR (C_6H_{12}, ν_{CO}, cm^{-1}): 2080 (m), 2032 (s), 2015 (m), 1992 (w), 1979 (m), 1910 (vs). $^{31}P\{^1H\}$ NMR (32.38 MHz, CD_2Cl_2, 300 K, δ (ppm)): –34.45 (s). ^1H NMR (80.00 MHz, CD_2Cl_2, 300 K, δ (ppm)): 7.43 (m, C_6H_5); 4.90 (d, P–CH=, $^2J_{PH}$ = 6 Hz); 1.23 (s, ^{t}Bu).

Preparation of Complex 2d from 2a. Complex **2a** (1 mmol, 0.72 g) was dissolved in 60 mL of THF, and the solution was cooled to –30 °C for the introduction of 1 mmol of 3,3-dimethylbutyne via a syringe. The reaction mixture was stirred at 50 °C for 6 h, until the monitoring of the reaction by infrared spectroscopy indicated that the ratio **2d**/**2a** remained constant. The products were chromatographed on a column of Florisil (eluant dichloromethane). From the first eluted fraction, dark red crystals of **2d**

Table I. Crystal Data, Intensity Collection, Reduction, and Refinement

	2a	2e	3a
formula	$C_{33}H_{20}O_7PCoRu$	$C_{24}H_{20}O_7PSiCoRu$	$C_{32}H_{20}O_6PCoRu\cdot0.5CH_2Cl_2$
mol wt	719.56	639.55	734.02
cryst syst	triclinic	monoclinic	monoclinic
space group	$P\bar{1}$	$I2/a$	$P2_1/c$
a, Å	8.280 (1)	17.054 (2)	17.041 (2)
b, Å	12.419 (2)	10.846 (2)	10.721 (1)
c, Å	14.966 (2)	30.671 (4)	17.511 (2)
α, deg	99.58 (1)	90	90
β, deg	99.55 (1)	107.81 (1)	101.56 (1)
γ, deg	90.10 (1)	90	90
Z	2	8	4
V, Å^3	1495.8 (4)	5401 (1)	3134.3 (5)
d(calcd), g/cm^3	1.597	1.573	1.555
μ(Mo Kα), cm^{-1}	11.73	13.28	12.00
radiation	graphite-monochromated Mo Kα (λ = 0.71609 Å)		
diffractometer	Syntex $P2_1$		
cryst size, mm	0.24 × 0.25 × 0.28	0.27 × 0.29 × 0.30	0.23 × 0.24 × 0.27
scan type	$\theta/2\theta$	$\theta/2\theta$	$\theta/2\theta$
2θ range, deg	≤50	≤46	≤45
scan speed, deg/min	2.55–29.3	3.45–29.30	2.93–29.30
scan width	0.8° below Kα_1 to 0.8° above Kα_2		
std rflns	137; 410	723; 0016	008; 800
change in stds, %	−2	−2	−2
no. of data measd	5281	3779	4132
no. of data obsd ($I \geq 3\sigma(I)$)	4191	3051	3465
transmissn factors	0.67–0.80	0.61–0.76	0.68–0.81
no. of variables	469	397	464
$R = \sum(\|F_o\| - \|F_c\|)/\sum\|F_o\|$	0.028	0.025	0.033
$R_w = [\sum w(\|F_o\| - \|F_c\|)^2/\sum w\|F_o\|^2]^{1/2}$	0.031	0.029	0.039
weighting scheme	$1.86 - 0.0342\|F_o\| + 0.00061\|F_o\|^2$	$2.1 - 0.028\|F_o\| + 0.00038\|F_o\|^2$	$2.96 - 0.0268\|F_o\| + 0.00044\|F_o\|^2$
electron dens level in final diff map, e/Å^3	0.51	0.28	0.82 (solvent Cl)

were isolated in 60% (0.40 g) yield. From the second fraction 0.18 g (25%) of complex **2a** was recovered.

Preparation of $(Ph_2PH)(CO)_2Ru\{\mu\text{-}\eta^3\text{-}Ph_2PCO(R^1)=C(R^2)\}Co(CO)_3$ (4). A solution was prepared with 0.5 mmol of complex **2** and 40 mL of THF and was stirred while 1 mmol (0.18 g) of diphenylphosphine was added with a syringe. The reaction was monitored by infrared spectra in cyclohexane solution or by thin-layer chromatography (eluant 1/1 dichloromethane–hexane). The solvent was removed under vacuum. Approximately 3–4 mL of Florisil and 10 mL of dichloromethane were added to the oily red reaction products; the heterogeneous mixture was stirred while dichloromethane was evaporated. The residual solid powder was placed at the top of a column of Florisil. Elution with a mixture of hexane and dichloromethane gave first a fraction containing the residual complex **2**, then a fraction containing a small amount of an unidentified product, and finally the complex **4**. Complexes **4** were recrystallized from a dichloromethane–hexane mixture.

4a ($R^1 = R^2 = Ph$). From 0.36 g (0.5 mmol) of **2a**, after 10 h of reaction at room temperature, the orange complex **4a** was isolated in 70% yield (0.30 g); mp 150–155 °C. IR (C_6H_{12}, ν_{CO}, cm^{-1}): 2040 (w), 2019 (vs), 1985 (m), 1969 (s), 1856 (m, broad), 1620 (w). $^{31}P\{^1H\}$ NMR (32.38 MHz, $CDCl_3$, 300 K, δ (ppm)): +42.80 (d, PCO); 23.88 (d, Ph_2PH); $^2J_{PP}$ = 256.3 Hz. ^{31}P NMR (δ (ppm)): 42.80 (d), 23.88 (dd, $^1J_{PH}$ = 366.0 Hz). ^1H NMR (300.13 MHz, $CDCl_3$, 300 K, δ (ppm)): 8.1–6.9 (m, C_6H_5); cis isomer (2%) 5.69 (dd, *PH*, $^1J_{PH}$ = 379.2 Hz, $^3J_{PH}$ = 3.2 Hz); trans isomer (98%) 5.24 (dd, PH, $^1J_{PH}$ = 375.5 Hz, $^3J_{PH}$ = 3.9 Hz).

4c ($R^1 = H$, $R^2 = Ph$). From 0.32 g (0.5 mmol) of **2c**, after either 12 h of reaction at 25 °C or 6 h of reaction at 50 °C, the orange complex **4c** was isolated in 60% yield (0.24 g); mp 160–165 °C. IR (C_6H_{12}, ν_{CO}, cm^{-1}): 2040 (w), 2021 (vs), 1984 (s), 1974 (s), 1870 (m, broad), 1618 (m). $^{31}P\{^1H\}$ NMR (32.38 MHz, $CDCl_3$, 300 K, δ (ppm)): trans isomer (62%) 42.27 (d, PCO), 29.31 (d, Ph_2PH, $^2J_{PP}$ = 253.9 Hz); cis isomer (38%) 44.97 (d, PCO), 13.57 (d, Ph_2PH, $^2J_{PP}$ = 21.9 Hz). ^{31}P NMR (δ (ppm)): trans isomer 42.27 (d), 29.31 (dd, $^1J_{PH}$ = 372.9 Hz); cis isomer 44.97 (d), 13.57 (dd, $^1J_{PH}$ = 373.1 Hz). ^1H NMR (300.13 MHz, $CDCl_3$, 300 K, δ (ppm)): 8.1–7.0 (m, C_6H_5); trans isomer 5.70 (d, =CH, $^3J_{PH}$ = 36.3 Hz), 5.10 (dd, PH, $^1J_{PH}$ = 372.9 Hz, $^3J_{PH}$ = 4.5 Hz); cis isomer 5.50 (dd, PH, $^1J_{PH}$ = 373.1 Hz, $^3J_{PH}$ = 7.2 Hz), 5.48 (dd, =CH, $^3J_{PH}$ = 37.8 Hz, $^4J_{PH}$ = 0.8 Hz).

4e ($R^1 = SiMe_3$, $R^2 = H$). From 0.32 g (0.5 mmol) of **2e**, after 6 h of reaction at 50 °C (no reaction occurred at 25 °C for 6 h), 0.24 g (60%) of complex **4e** was obtained; mp 160–165 °C dec. IR (C_6H_{12}, ν_{CO}, cm^{-1}): 2041 (w), 2022 (vs), 1983 (s), 1974 (s), 1863 (m, broad), 1616 (w). $^{31}P\{^1H\}$ NMR (32.38 MHz, $CDCl_3$, 300 K, δ (ppm)): trans isomer (95%) 50.05 (d, PCO), 26.14 (d, Ph_2PH), $^2J_{PP}$ = 249.0 Hz; cis isomer (5%) 48.41 (d, PCO), 26.79 (d, Ph_2PH), $^2J_{PP}$ = 24.9 Hz. ^{31}P NMR (δ (ppm)): trans isomer 50.05 (d), 26.14 (dd, $^1J_{PH}$ = 368.3 Hz). The $^1J_{PH}$ value for the cis isomer was not observed due to the weak intensity of the signals. ^1H NMR (300.13 MHz, $CDCl_3$, 300 K, δ (ppm)): 8.3–7.0 (m, C_6H_5); trans isomer 5.88 (dd, Ph_2PH, $^1J_{PH}$ = 364.0 Hz, $^3J_{PH}$ = 3.1 Hz), 0.07 (s, $SiMe_3$); cis isomer 5.23 (dd, Ph_2PH, $^1J_{PH}$ = 386.0 Hz, $^3J_{PH}$ = 12.5 Hz), 0.09 (s, $SiMe_3$). The alkyne proton was masked by the phenyl proton signals.

X-ray Structure Analyses. Collection and Reduction of X-ray Data. Crystals of **2a** were grown from CH_2Cl_2–hexane as orange-yellow prisms. Recrystallization of **2e** from *n*-hexane afforded orange prisms, and crystals of **3a** were obtained from *n*-hexane as orange-yellow hexagonal prisms. A suitable crystal was attached to a goniometer head via a glass fiber on a brass pin and mounted on a Syntex $P2_1$, Data General Nova controlled automatic diffractometer for preliminary examination. Polaroid rotation photographs in combinations with the Syntex autoindexing and cell refinement procedures were used to identify possible unit cells. Space group and crystal data for cells refined with 15 reflections well dispersed in reciprocal space are given in Table I. For complex **2a**, the choice of the centric space group $P\bar{1}$ was initially based on centric E statistics and a Patterson map consistent with single occupancy of the asymmetric unit. The choice of space group $I2/a$ rather than acentric Ia was based on similar reasoning. The correctness of both of these assignments was confirmed by the solution and refinement of the structures.

Intensity data were collected on the $P2_1$ diffractometer for appropriate crystals as indicated in Table I. Intensities were measured via $\theta/2\theta$ scans with a variable scan rate set to optimize measurements on weak and strong reflections. Background measurements were made at the beginning and end of each scan for a time equal to half of the total scan. For each crystal, instrumental and compound stability were monitored by measurement of two standard reflections after every 100 reflections. None of the three compounds exhibited any significant decay over the period of data collection. Measured reflections were flagged as unobserved when $I \leq 3\sigma(I)$, where σ was determined from counting statistics. Data were corrected for Lorentz and polar-

Table II. Atomic Positional Parameters (Fractional, ×10⁴) for 2a

atom	x	y	z
Ru	730.6 (3)	2256.2 (2)	2221.0 (2)
Co	3415.6 (5)	1082.6 (3)	2321.8 (3)
P	2624.0 (10)	3226.2 (6)	1643.6 (5)
O(1)	-1799 (3)	2237 (3)	456 (2)
O(2)	-1528 (3)	784 (3)	2986 (2)
O(3)	-421 (4)	4394 (2)	3202 (2)
O(4)	5723 (4)	752 (2)	1019 (2)
O(5)	812 (3)	-163 (2)	1058 (2)
O(6)	4246 (4)	-804 (2)	3215 (2)
O(7)	5901 (3)	3370 (2)	2212 (2)
C(1)	-898 (4)	2216 (3)	1105 (2)
C(2)	-680 (4)	1335 (3)	2746 (2)
C(3)	-30 (4)	3595 (3)	2838 (2)
C(4)	4791 (4)	896 (3)	1491 (3)
C(5)	1596 (4)	512 (3)	1571 (2)
C(6)	3912 (5)	-44 (3)	2912 (2)
C(7)	4608 (4)	3067 (2)	2400 (2)
C(8)	2789 (4)	2235 (2)	3304 (2)
C(9)	4376 (4)	2600 (2)	3207 (2)
C(10)	2515 (4)	2136 (3)	4253 (2)
C(11)	1989 (4)	1172 (3)	4483 (2)
C(12)	1830 (5)	1106 (4)	5381 (3)
C(13)	2163 (5)	2011 (4)	6055 (3)
C(14)	2630 (5)	2983 (4)	5833 (3)
C(15)	2810 (4)	3046 (3)	4940 (2)
C(16)	5807 (4)	2724 (3)	3975 (2)
C(17)	6313 (4)	1903 (3)	4466 (2)
C(18)	7577 (5)	2082 (4)	5205 (3)
C(19)	8364 (5)	3089 (4)	5470 (3)
C(20)	7891 (5)	3905 (3)	4983 (3)
C(21)	6627 (5)	3724 (3)	4246 (3)
C(22)	2336 (4)	4695 (2)	1772 (2)
C(23)	3345 (5)	5442 (3)	2405 (3)
C(24)	3026 (6)	6543 (3)	2502 (3)
C(25)	1707 (6)	6904 (3)	1982 (3)
C(26)	686 (7)	6178 (4)	1356 (4)
C(27)	990 (6)	5077 (3)	1247 (3)
C(28)	3031 (4)	2880 (2)	475 (2)
C(29)	2284 (4)	2002 (3)	-135 (2)
C(30)	2699 (5)	1748 (3)	-1010 (2)
C(31)	3865 (6)	2372 (4)	-1256 (3)
C(32)	4617 (6)	3250 (4)	-651 (3)
C(33)	4207 (5)	3514 (3)	213 (3)

ization effects, but with small values of μ(Mo Kα) no corrections for absorption were deemed necessary. Observed intensities were reduced to structure factors in the normal way.

Solution and Refinement of X-ray Data. All three structures were solved by heavy-atom methods, the cobalt and ruthenium atoms being identified in Patterson maps and light atoms via subsequent Fourier syntheses. Least-squares refinement of positions and isotropic thermal parameters for non-hydrogen atoms afforded R values ($R = \sum||F_o| - |F_c||/\sum|F_o|$) of 0.62 for **2a**, 0.077 for **2e**, and 0.076 for **3a**. Conversion to anisotropic temperature factors and further cycles of refinement followed by a difference Fourier calculation in each case allowed the identification of all hydrogen atoms in the three molecules. In subsequent refinement to convergence hydrogens were included and isotropic temperature factors refined. For complex **3a**, the asymmetric unit contains a half molecule of the solvent of crystallization (CH_2Cl_2) disordered about an inversion center. Carbon atom C(33) was refined with 50% occupancy. Appropriate weighting schemes (Table I) were used in the final cycles. Final difference maps were featureless, with residual electron density levels listed in Table I. Final R and R_w ($R_w = [\sum w(|F_o| - |F_c|)^2/\sum w|F_o|^2]^{1/2}$) values for **2a**, **2e**, and **3a** were respectively 0.028 and 0.031, 0.025 and 0.029, and 0.033 and 0.039 All calculations used the full matrix and were carried out on IBM 4341 systems in the University of Waterloo Computer Centre. Scattering factors for heavy atoms were taken from ref 19 and for hydrogen atoms from the data of Stewart et al.[20] Programs used in the calculations are those described

(19) *International Tables for X-ray Crystallography*; Kynoch Press: Birmingham, England, 1974; Vol. IV.

Table III. Selected Bond Lengths (Å) for 2a

Ru-Co	2.6577 (4)	Ru-P	2.3335 (8)
Ru-C(1)	1.958 (3)	Ru-C(2)	1.972 (4)
Ru-C(3)	1.923 (4)	Ru-C(5)	2.380 (4)
Ru-C(8)	2.152 (3)	Co-C(4)	1.809 (4)
Co-C(5)	1.789 (4)	Co-C(6)	1.788 (4)
Co-C(8)	2.008 (3)	Co-C(9)	2.180 (3)
P-C(7)	1.865 (3)	P-C(22)	1.822 (3)
P-C(28)	1.818 (3)	C(1)-O(1)	1.128 (4)
C(2)-O(2)	1.121 (5)	C(3)-O(3)	1.126 (5)
C(4)-O(4)	1.125 (5)	C(5)-O(5)	1.157 (5)
C(6)-O(6)	1.129 (4)	C(7)-O(7)	1.225 (4)
C(7)-C(9)	1.463 (4)	C(8)-C(9)	1.426 (4)
C(8)-C(10)	1.500 (4)	C(9)-C(16)	1.496 (4)

Table IV. Selected Bond Angles (deg) for 2a

Co-Ru-P	74.68 (2)	Co-Ru-C(1)	124.3 (1)
Co-Ru-C(2)	99.3 (1)	Co-Ru-C(3)	138.6 (1)
Co-Ru-C(5)	41.1 (1)	Co-Ru-C(8)	47.9 (1)
P-Ru-C(1)	92.0 (1)	P-Ru-C(2)	174.0 (1)
P-Ru-C(3)	90.8 (1)	P-Ru-C(5)	94.1 (1)
P-Ru-C(8)	81.6 (1)	C(1)-Ru-C(2)	92.1 (1)
C(1)-Ru-C(3)	94.1 (1)	C(1)-Ru-C(5)	88.3 (1)
C(1)-Ru-C(8)	171.1 (1)	C(2)-Ru-C(3)	93.3 (1)
C(2)-Ru-C(5)	81.6 (1)	C(2)-Ru-C(8)	93.8 (1)
C(3)-Ru-C(5)	174.5 (1)	C(3)-Ru-C(8)	92.2 (1)
C(5)-Ru-C(8)	85.9 (1)	Ru-Co-C(4)	125.9 (1)
Ru-Co-C(5)	61.1 (1)	Ru-Co-C(6)	129.2 (1)
Ru-Co-C(8)	52.5 (1)	Ru-Co-C(9)	79.9 (1)
C(4)-Co-C(5)	97.8 (1)	C(4)-Co-C(6)	101.4 (1)
C(4)-Co-C(8)	140.0 (1)	C(4)-Co-C(9)	102.1 (1)
C(5)-Co-C(6)	98.9 (1)	C(5)-Co-C(8)	108.9 (1)
C(5)-Co-C(9)	140.7 (1)	C(6)-Co-C(8)	103.1 (1)
C(6)-Co-C(9)	109.7 (1)	C(8)-Co-C(9)	39.6 (1)
Ru-P-C(7)	103.8 (1)	Ru-P-C(22)	114.9 (1)
Ru-P-C(28)	123.1 (1)	C(7)-P-C(22)	105.1 (1)
C(7)-P-C(28)	105.5 (1)	C(22)-P-C(28)	102.9 (1)
Ru-C(1)-O(1)	176.6 (1)	Ru-C(2)-O(2)	175.4 (1)
Ru-C(3)-O(3)	177.6 (1)	Co-C(4)-O(4)	175.1 (1)
Ru-C(5)-Co	77.8 (1)	Ru-C(5)-O(5)	127.5 (1)
Co-C(5)-O(5)	154.6 (1)	Co-C(6)-O(6)	174.2 (1)
P-C(7)-O(7)	120.5 (1)	P-C(7)-C(9)	112.0 (1)
C(9)-C(7)-O(7)	127.4 (1)	Ru-C(8)-Co	79.3 (1)
Ru-C(8)-C(9)	120.5 (1)	Ru-C(8)-C(10)	120.1 (1)
Co-C(8)-C(9)	76.7 (1)	Co-C(8)-C(10)	129.1 (1)
C(9)-C(8)-C(10)	117.4 (1)	Co-C(9)-C(7)	90.2 (1)
Co-C(9)-C(8)	63.7 (1)	Co-C(9)-C(16)	126.6 (1)
C(7)-C(9)-C(8)	120.6 (1)	C(7)-C(9)-C(16)	115.8 (1)
C(8)-C(9)-C(16)	122.7 (1)		

elsewhere.[21] For the three molecules **2a**, **2e**, and **3a**, respectively, atomic positional parameters are listed in Tables II, V, and VIII along with compilations of pertinent bond lengths (Tables III, VI, and IX) and angles (Tables IV, VII, and X). Anisotropic thermal parameters (Tables S1, S4, and S7), hydrogen atomic positions and isotropic thermal parameters (Tables S2, S5, and S8), and additional bond lengths and angles (Tables S3, S6, and S9) are available as supplementary data,[22] as are structure factors for the three molecules (Tables S10, S11, and S12).

Results and Discussion

Synthesis and Spectroscopic Properties of Complexes 2a–f. The phosphido-bridged carbonyl complex **1** reacts readily with mono- and disubstituted alkynes at 35 °C in THF as shown in Scheme I. The principal products formed under these mild conditions are the yellow-orange complexes **2a–f**. For the alkynes $R^1C{\equiv}CR^2$ ($R^1 = R^2 = Ph$; $R^1 = Ph$, $R^2 = C{\equiv}CPh$; $R^1 = Ph$, $R^2 = H$; $R^1 = {}^tBu$, $R^2 = H$) smaller amounts of the second products **3a–d** were also obtained. At 65 °C, the complexes **3a–d** were the major products. Subsequent experiments con-

(20) Stewart, R. F.; Davidson, E. R.; Simpson, W. T. *J. Chem. Phys.* **1965**, *42*, 3175.

(21) Carty, A. J.; Mott, G. N.; Taylor, N. J.; Yule, J. E. *J. Am. Chem. Soc.* **1978**, *100*, 35.

(22) See paragraph on supplementary material at the end of the paper.

Table V. Atomic Positional Parameters (Fractional, ×10⁴) for 2e

atom	x	y	z
Ru	3509.2 (2)	1852.6 (3)	1257.0 (1)
Co	2910.1 (3)	-414.3 (5)	1278.6 (2)
P	2104.4 (5)	2029.4 (8)	833.0 (3)
Si	1691.1 (7)	-136.0 (10)	2020.7 (4)
O(1)	4258 (2)	2596 (3)	496 (1)
O(2)	5134 (2)	1087 (3)	1968 (1)
O(3)	3564 (2)	4436 (3)	1641 (1)
O(4)	3914 (2)	-475 (3)	679 (1)
O(5)	3826 (3)	-2320 (4)	1900 (2)
O(6)	1613 (2)	-1685 (3)	570 (1)
O(7)	859 (1)	893 (2)	1047.0 (8)
C(1)	3980 (2)	2341 (4)	770 (1)
C(2)	4563 (2)	1393 (4)	1693 (1)
C(3)	3545 (2)	3477 (4)	1501 (1)
C(4)	3555 (2)	-224 (4)	929 (1)
C(5)	3466 (3)	-1563 (5)	1672 (2)
C(6)	2104 (3)	-1195 (4)	845 (2)
C(7)	1592 (2)	1057 (3)	1178 (1)
C(8)	2992 (2)	982 (3)	1717 (1)
C(9)	2161 (2)	622 (3)	1608 (1)
C(10)	1137 (4)	-1564 (5)	1771 (2)
C(11)	964 (4)	993 (6)	2149 (2)
C(12)	2526 (3)	-502 (6)	2553 (2)
C(13)	1604 (2)	3516 (3)	829 (1)
C(14)	1321 (2)	4213 (4)	436 (1)
C(15)	944 (3)	5336 (4)	446 (1)
C(16)	845 (3)	5770 (4)	843 (2)
C(17)	1123 (3)	5092 (4)	1237 (2)
C(18)	1503 (3)	3968 (4)	1230 (1)
C(19)	1696 (2)	1521 (3)	242 (1)
C(20)	2197 (2)	1332 (4)	-31 (1)
C(21)	1857 (3)	998 (5)	-486 (1)
C(22)	1023 (3)	845 (4)	-665 (1)
C(23)	524 (2)	1021 (4)	-397 (1)
C(24)	854 (2)	1364 (4)	53 (1)

Table VI. Selected Bond Lengths (Å) for 2e

Ru-Co	2.6710 (6)	Ru-P	2.3583 (9)
Ru-C(1)	1.973 (4)	Ru-C(2)	1.949 (4)
Ru-C(3)	1.908 (4)	Ru···C(4)	2.477 (4)
Ru-C(8)	2.102 (4)	Co-C(4)	1.766 (4)
Co-C(5)	1.790 (5)	Co-C(6)	1.805 (4)
Co-C(8)	2.001 (4)	Co-C(9)	2.170 (3)
P-C(7)	1.887 (3)	P-C(13)	1.822 (3)
P-C(19)	1.818 (3)	C(1)-O(1)	1.118 (5)
C(2)-O(2)	1.126 (5)	C(3)-O(3)	1.122 (5)
C(4)-O(4)	1.153 (5)	C(5)-O(5)	1.131 (7)
C(6)-O(6)	1.124 (6)	C(7)-O(7)	1.219 (4)
C(7)-C(9)	1.456 (5)	C(8)-O(9)	1.409 (5)
C(9)-Si	1.881 (3)	Si-C(10)	1.853 (6)
Si-C(11)	1.868 (7)	Si-C(12)	1.851 (5)

firmed that **2a–d** but not **2e,f** were converted to compounds of type **3** at 60–65 °C via decarbonylation.

The new heterobimetallics **2** exhibit four terminal ν_{CO} infrared frequencies and bands in the regions 1878–1900 and 1602–1625 cm^{-1} due to bridging carbonyls and ketonic CO groups, respectively. The $^{31}P\{^1H\}$ shifts of **2** (+37.4–50.5 ppm) lie well upfield of the value (+185.0 ppm) for the parent compound $RuCo(CO)_7(\mu\text{-}PPh_2)$, suggesting either the loss of the metal–metal bond[23] of the latter or the transformation of the phosphido group to a phosphine ligand. Furthermore, the ^{31}P resonances show no evidence of line broadening induced by the ^{59}Co quadrupole as frequently observed for cobalt-coordinated phosphorus ligands and seen in the precursor **1**.[7] The cleavage of the Co–P bond in **1** on conversion to **2** was subsequently confirmed by single-crystal X-ray analyses of **2a** and **2e**.

(23) Carty, A. J.; MacLaughlin, S. A.; Nucciarone, D. In *Phosphorus-31 NMR Spectroscopy in Stereochemical Analysis: Organic Compounds and Metal Complexes*; Verkade, J. G., Quin, L. D., Eds.; VCH: New York, 1986; Chapter 16, p 559–619.

Table VII. Selected Bond Angles (deg) for 2e

Co-Ru-P	75.93 (2)	Co-Ru-C(1)	120.9 (1)
Co-Ru-C(2)	91.6 (1)	Co-Ru-C(3)	143.8 (1)
Co-Ru-C(8)	47.8 (1)	P-Ru-C(1)	98.1 (1)
P-Ru-C(2)	165.4 (1)	P-Ru-C(3)	92.6 (1)
P-Ru-C(8)	80.9 (1)	C(1)-Ru-C(2)	94.9 (2)
C(1)-Ru-C(3)	94.4 (2)	C(1)-Ru-C(8)	168.6 (1)
C(2)-Ru-C(3)	93.2 (2)	C(2)-Ru-C(8)	85.0 (2)
C(3)-Ru-C(8)	97.0 (1)	Ru-Co-C(4)	64.1 (1)
Ru-Co-C(5)	122.0 (2)	Ru-Co-C(6)	128.7 (1)
Ru-Co-C(8)	51.1 (1)	Ru-Co-C(9)	79.6 (1)
C(4)-Co-C(5)	101.0 (2)	C(4)-Co-C(6)	94.8 (2)
C(4)-Co-C(8)	113.0 (2)	C(4)-Co-C(9)	141.9 (2)
C(5)-Co-C(6)	107.3 (2)	C(5)-Co-C(8)	99.2 (2)
C(5)-Co-C(9)	108.2 (2)	C(6)-Co-C(8)	137.0 (2)
C(6)-Co-C(9)	99.3 (2)	C(8)-Co-C(9)	39.2 (1)
Ru-P-C(7)	102.2 (1)	Ru-P-C(13)	118.1 (1)
Ru-P-C(19)	122.7 (1)	C(7)-P-C(13)	101.7 (1)
C(7)-P-C(19)	106.7 (1)	C(13)-P-C(19)	103.0 (2)
C(9)-Si-C(10)	110.8 (2)	C(9)-Si-C(11)	107.6 (2)
C(9)-Si-C(12)	108.4 (2)	C(10)-Si-C(11)	110.3 (3)
C(10)-Si-C(12)	110.0 (3)	C(1)-Si-C(12)	109.7 (3)
Ru-C(1)O(1)	178.5 (2)	Ru-C(2)-O(2)	174.0 (2)
Ru-C(3)-O(3)	179.6 (2)	Ru···C(4)-Co	76.0 (1)
Ru···C(4)-O(4)	125.1 (1)	Co-C(4)-O(4)	159.0 (1)
Co-C(5)-C(5)	176.1 (3)	Co-C(6)-O(6)	178.6 (2)
P-C(7)-O(7)	120.6 (1)	P-C(7)-C(9)	113.3 (1)
O(7)-C(7)-C(9)	126.1 (2)	Ru-C(8)-Co	81.2 (1)
Ru-C(8)-C(9)	124.3 (1)	Co-C(8)-C(9)	76.9 (1)
Co-C(9)-Si	121.3 (1)	Co-C(9)-C(7)	94.0 (1)
Co-C(9)-C(8)	63.9 (1)	Si-C(9)-C(7)	116.7 (1)
Si-C(9)-C(8)	124.5 (1)	C(7)-C(9)-C(8)	117.9 (2)

Scheme I

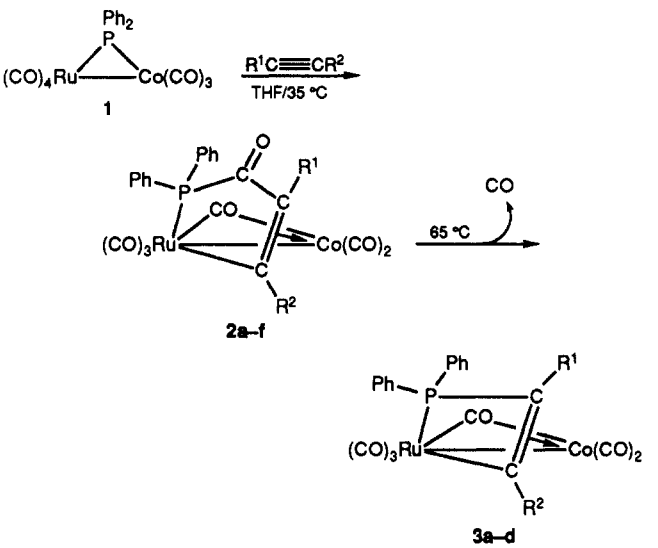

R^1, R^2 = Ph, Ph (**a**), Ph, C≡CPh (**b**), H, Ph (**c**), H, ^{t}Bu (**d**), $SiMe_3$, H (**e**), H, H (**f**)

Chart I

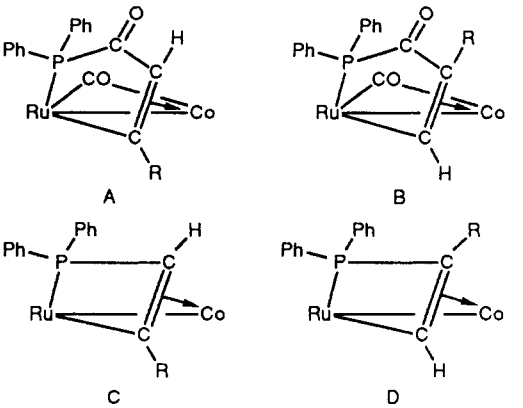

Table VIII. Atomic Positional Parameters (Fractional, ×10⁴) for 3a

atom	x	y	z
Ru	3388.5 (2)	2272.3 (4)	2363.5 (2)
Co	3805.3 (4)	1373.1 (6)	3795.9 (4)
P	2509.9 (7)	3007.0 (12)	3146.9 (7)
O(1)	2047 (3)	1979 (5)	956 (2)
O(2)	4059 (3)	4732 (4)	1835 (3)
O(3)	4580 (3)	721 (4)	1646 (3)
O(4)	3872 (3)	2473 (5)	5330 (2)
O(5)	4542 (3)	-1036 (5)	4232 (3)
O(6)	5168 (2)	2744 (5)	3501 (3)
C(1)	2561 (3)	2121 (5)	1474 (3)
C(2)	3830 (4)	3831 (5)	2037 (3)
C(3)	4133 (3)	1280 (5)	1907 (3)
C(4)	3858 (3)	2086 (6)	4727 (3)
C(5)	4244 (3)	-112 (6)	4039 (4)
C(6)	4569 (3)	2249 (6)	3493 (3)
C(7)	2913 (2)	794 (4)	2951 (2)
C(8)	2543 (2)	1426 (4)	3512 (2)
C(9)	2723 (3)	-467 (4)	2638 (3)
C(10)	1939 (3)	-879 (5)	2488 (3)
C(11)	1743 (4)	-2047 (6)	2145 (4)
C(12)	2317 (5)	-2800 (6)	1952 (4)
C(13)	3084 (4)	-2392 (6)	2088 (4)
C(14)	3295 (4)	-1244 (5)	2429 (3)
C(15)	2079 (3)	868 (5)	4066 (3)
C(16)	2280 (3)	-297 (6)	4394 (3)
C(17)	1866 (4)	-819 (7)	4921 (4)
C(18)	1247 (4)	-168 (7)	5138 (4)
C(19)	1032 (3)	961 (6)	4818 (3)
C(20)	1439 (3)	1473 (5)	4272 (3)
C(21)	1489 (3)	3408 (5)	2654 (3)
C(22)	977 (3)	2483 (6)	2309 (4)
C(23)	224 (4)	2780 (7)	1880 (4)
C(24)	-16 (3)	3978 (6)	1794 (4)
C(25)	481 (4)	4897 (7)	2130 (4)
C(26)	1230 (4)	4625 (5)	2566 (3)
C(27)	2797 (3)	4262 (5)	3853 (3)
C(28)	2378 (4)	4528 (6)	4423 (4)
C(29)	2631 (5)	5457 (6)	4964 (4)
C(30)	3289 (4)	6145 (7)	4934 (4)
C(31)	3720 (5)	5888 (7)	4371 (5)
C(32)	3475 (4)	4953 (7)	3839 (4)
C(33)[a]	507 (16)	5968 (27)	5069 (17)
Cl	-54 (4)	4424 (6)	4302 (3)

[a] Solvent atom with occupancy 0.5.

Table IX. Selected Bond Lengths (Å) for 3a

Ru-Co	2.6479 (7)	Ru-P	2.359 (1)
Ru-C(1)	1.887 (5)	Ru-C(2)	1.964 (6)
Ru-C(3)	1.946 (5)	Ru···C(6)	2.523 (6)
Ru-C(7)	2.136 (4)	Co-C(4)	1.786 (5)
Co-C(5)	1.774 (6)	Co-C(6)	1.771 (6)
Co-C(7)	1.997 (4)	Co-C(8)	2.110 (4)
P-C(8)	1.809 (5)	P-C(21)	1.832 (5)
P-C(27)	1.826 (5)	C(1)-O(1)	1.138 (7)
C(2)-O(2)	1.126 (7)	C(3)-O(3)	1.135 (7)
C(4)-O(4)	1.130 (7)	C(5)-O(8)	1.134 (8)
C(6)-O(6)	1.147 (7)	C(7)-C(8)	1.440 (6)
C(7)-C(9)	1.470 (6)	C(8)-C(15)	1.494 (6)

The proton NMR spectra of **2f** ($R^1 = R^2 = H$) consisted of three phenyl multiplets at 7.25–7.95 ppm and ethylenic resonances appearing as a doublet of doublets at 5.43 ppm with J_{PH} = 38 Hz and J_{HH} = 1.1 Hz and a low-field doublet at 8.19 Hz with J_{HH} = 1.1 Hz. For the unsymmetrical alkyne insertion products **2b–e** the two regioisomers A and B (Chart I), differing in the orientation of the substituents R^1 and R^2, are possible. Proton NMR spectra on the purified products suggested, however, the presence of a unique stereoisomer for each of the compounds **2b–e** with **2c,d** having one configuration, the trimethylsilyl derivative **2e** having the other, and the structure of **2b** (R^1 = Ph, R^2 = C≡CPh) being indeterminate. Thus, for **2e** (R^1, R^2 = $SiMe_3$, H) only a low-field olefinic resonance at 8.65 ppm

Table X. Selected Bond Angles (deg) for 3a

Co-Ru-P	69.62 (3)	Co-Ru-C(1)	139.9 (1)
Co-Ru-C(2)	122.7 (1)	Co-Ru-C(3)	96.7 (1)
Co-Ru-C(7)	47.9 (1)	P-Ru-C(1)	93.0 (1)
P-Ru-C(2)	102.1 (1)	P-Ru-C(3)	164.4 (1)
P-Ru-C(7)	67.8 (1)	C(1)-Ru-C(2)	95.7 (2)
C(1)-Ru-C(3)	93.2 (2)	C(1)-Ru-C(7)	92.3 (2)
C(2)-Ru-C(3)	91.5 (2)	C(2)-Ru-C(7)	167.5 (2)
C(3)-Ru-C(7)	97.7 (1)	Ru-Co-C(4)	131.6 (1)
Ru-Co-C(5)	125.1 (1)	Ru-Co-C(6)	66.2 (1)
Ru-Co-C(7)	52.5 (1)	Ru-Co-C(8)	72.5 (1)
C(4)-Co-C(5)	102.9 (2)	C(4)-Co-C(6)	98.1 (2)
C(4)-Co-C(7)	134.5 (2)	C(4)-Co-C(8)	93.8 (2)
C(5)-Co-C(6)	104.4 (2)	C(5)-Co-C(7)	96.9 (2)
C(5)-Co-C(8)	116.2 (2)	C(6)-Co-C(7)	116.1 (2)
C(6)-Co-C(8)	133.8 (2)	C(7)-Co-C(8)	40.9 (1)
Ru-P-C(8)	85.1 (1)	Ru-P-C(21)	117.2 (1)
Ru-P-C(27)	121.6 (1)	C(8)-P-C(21)	110.2 (2)
C(8)-P-C(27)	117.8 (2)	C(21)-P-C(27)	104.3 (2)
Ru-C(1)-O(1)	176.5 (2)	Ru-C(2)-O(2)	177.7 (2)
Ru-C(3)-O(3)	178.4 (2)	Co-C(4)-O(4)	175.8 (2)
Co-C(5)-O(5)	176.4 (2)	Ru-C(6)-Co	73.8 (1)
Ru-C(6)-O(6)	125.0 (2)	Co-C(6)-O(6)	161.2 (2)
Ru-C(7)-Co	79.6 (1)	Ru-C(7)-C(8)	103.9 (1)
Ru-C(7)-C(9)	125.4 (1)	Co-C(7)-C(8)	73.8 (1)
Co-C(7)-C(9)	129.8 (1)	C(8)-C(7)-C(9)	126.4 (2)
Co-C(8)-P	93.8 (1)	Co-C(8)-C(7)	65.3 (1)
Co-C(8)-C(15)	118.9 (1)	P-C(8)-C(7)	100.7 (1)
P-C(8)-C(15)	128.4 (1)	C(7)-C(8)-C(15)	128.1 (2)

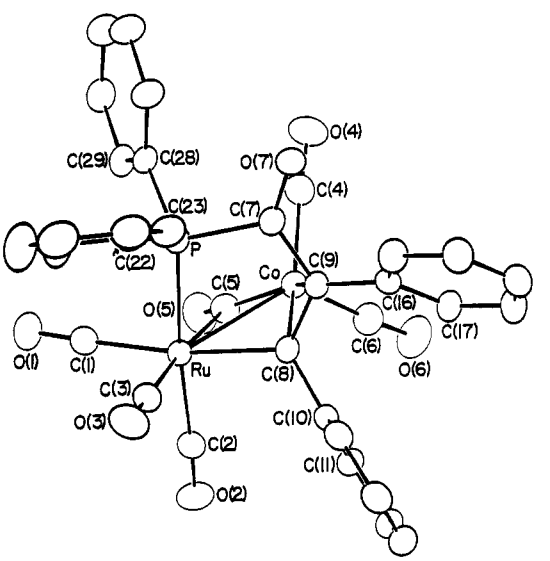

Figure 1. Molecular structure of $(CO)_3Ru(\mu\text{-}Ph_2PC(O)C(Ph)=C(Ph))Co(CO)_3$ (**2a**).

with a small J_{PH} value of 1.3 Hz was observed, while for **2c** and **2d** the olefinic signal was at high field (**2c**, 5.43 ppm; **2d**, 5.44 ppm) and the P–H coupling constant was large (**2c**, J_{PH} = 38.3 Hz; **2d**, J_{PH} = 38.3 Hz). Since **2e** was uniquely identified by X-ray analysis (vide infra) as having configuration B with the $SiMe_3$ substituent adjacent to the ketonic carbonyl, **2c** and **2d** must have structure A. Clearly an olefinic proton α to the ruthenium atom in complexes of type **2** is significantly deshielded. The large difference in three-bond P–H coupling constants between regioisomers A and B (>37 Hz) is also notable. The small value of $^3J_{PH}$ in **2e** and the correspondingly small value in **2f** may reflect a poorer transmission of electronic effects through the metal than through the organic framework of the ligand, a difference in P–M–C–H and P–C–C–H dihedral angles, a sum of positive and negative contributions to J_{PH}, or a combination of these effects.

X-ray Structures of 2a and 2e. The molecular structures of **2a** and **2e** are illustrated in Figures 1 and 2, respectively. The principal structural features of the two

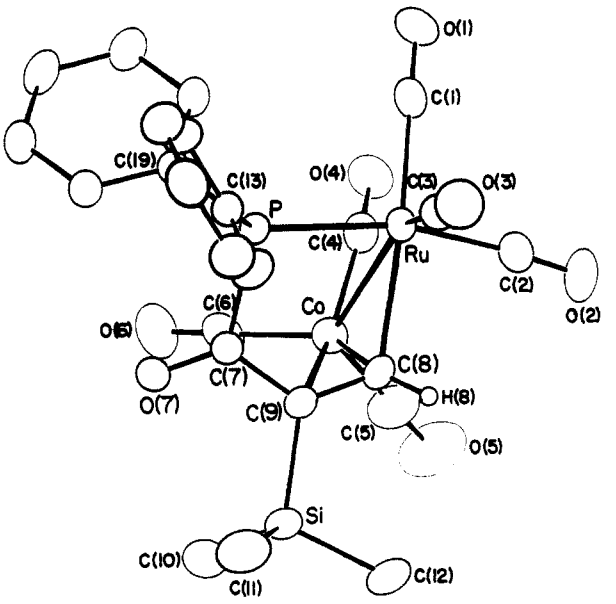

Figure 2. Molecular structure of $(CO)_3Ru(\mu\text{-}Ph_2PC(O)C(SiMe_3)=C(H))Co(CO)_3$ (**2e**).

molecules are closely similar, with the two metal atoms linked by a strong Ru–Co bond (Ru–Co = 2.6577 (4) Å (**2a**), 2.6710 (6) Å (**2e**)), an asymmetric bridging carbonyl, and a new unsaturated α-carbonylphosphine ligand derived from the coupling of the phosphido bridge, a carbonyl group, and the alkyne. The $Ph_2PC(O)C(R^1)=C(R^2)$– ligand is coordinated to the ruthenium atom in each complex as a tertiary phosphine with the alkenyl carbon atom C(8) also attached to the same metal such that a five-membered P–C(7)–C(9)–C(8)–Ru chelate ring is formed. The double bond of the chelate ring is bound in an η^2 fashion to the $Co(CO)_3$ moiety with the coordinated C(8)–C(9) bond length (1.426 (4) Å in **2a**, 1.409 (5) Å in **2e**) being typical for olefin–metal complexes.[24] The P–C(7)–C(9)–C(8) moiety in each complex is almost planar, with the ruthenium atom slightly below this plane. The stereochemistry at each ruthenium atom is distorted octahedral if the Ru–Co bond is considered to occupy a site trans to C(3)–O(3). Although the cobalt atoms in **2a** and **2e** have bonding contacts to six atoms, the stereochemistry is quite irregular and is probably best described as an "allyl-like" Ru–C(8)–C(7) fragment attached to a trigonal $Co(CO)_3$ unit. In terms of overall electron counting both metal atoms achieve an 18-electron configuration.

A notable feature of both compounds is the elongated phosphorus–carbon bond to the ketonic carbon atom. The P–C(7) distances 1.865 (3) Å in **2a** and 1.887 (3) Å in **2e** are significantly longer than expected for $P\text{–}C_{sp^2}$ bond lengths. Comparison with the average P–C(phenyl) bond lengths (1.820 Å in **2a**, 1.822 Å in **2e**) indicates a lengthening of 0.04–0.06 Å over the expected values, possibly due to ring strain in the five-membered chelate ring.

In the trimethylsilyl compound **2e** the Me_3Si substituent lies adjacent to the ketone group C(7)–O(7) with the unsubstituted alkyne carbon atom C(8) bound to ruthenium. Although this orientation has only a small influence on the molecular parameters for the P–C(7)–C(9)–C(8) fragment, there is a significantly shorter Ru–C(8) bond (2.102 (4) Å) in **2e** than in **2a** (Ru–C(8) = 2.152 (3) Å), which is most likely attributable to relief of steric pressure on substitution of a bulky phenyl group at C(8) in **2a** for a hydrogen atom in **2e**.

(24) Ittel, S. D.; Ibers, J. A. *Adv. Organomet. Chem.* **1976**, *14*, 33.

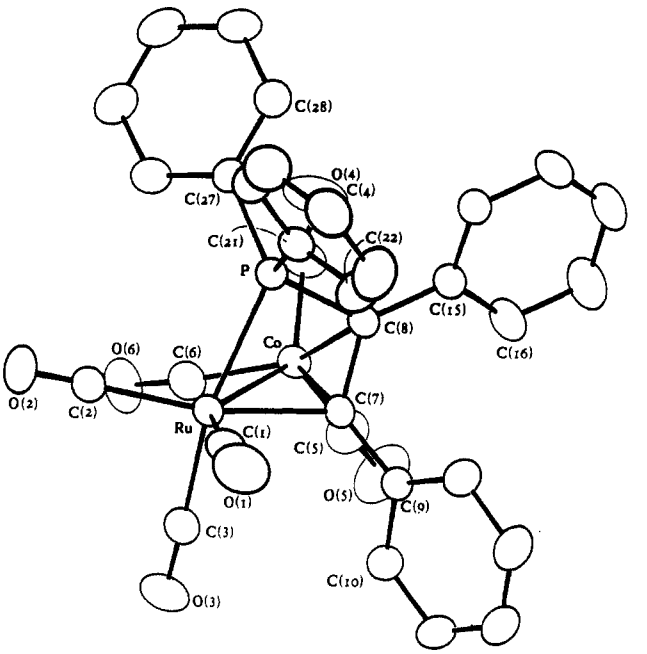

Figure 3. Molecular structure of $(CO)_3Ru(\mu\text{-}Ph_2PC(Ph)=C(Ph))Co(CO)_3$ (**3a**).

Conversion of Complexes 2 to Complexes 3. When complexes **2a–d** are heated in THF for 6 h at 60–65 °C, decarbonylation occurs, affording moderate (50–60%) yield of the new complexes **3a–d**. Similar yields of **3** can be obtained directly from **1** and the alkyne under analogous conditions. In contrast, **2e** and **2f** did not undergo CO extrusion in refluxing THF.

The loss of a carbonyl group in the transformation **2a–d** → **3a–d** was evident in infrared spectra of the products, which lacked the ketonic ν_{CO} frequency near 1600 cm^{-1} in **2a–d**. The $^{31}P\{^1H\}$ NMR spectra of **3a–d** exhibited singlet resonances well upfield ($\Delta\delta = \delta_{^{31}P}(\mathbf{3a}) - \delta_{^{31}P}(\mathbf{2a}) = 67.2$ ppm) of the corresponding shifts in **2a–d**. These shifts are consistent with the loss of a carbonyl group from the five-membered ring in **2a–d** and the formation of a four-membered P–C–C–Ru ring in **3a–d**. Ring shift contributions ΔR to $\delta_{^{31}P}$ are known to be negative for four-membered chelate rings containing phosphorus.[25] For example in the case of the hexacoordinate iridium complex Ir–CH(Me)$CH_2P^tBu_2$(H)(Cl)(L)($^tBu_3P$)[26] a ΔR value of –41.5 ppm has been attributed to the four-membered Ir–C–C–P ring.

For the unsymmetrical alkyne products **2c** and **2d** decarbonylation gave single regioisomers with double ^1H NMR resonances at 5.10 ppm ($^2J_{PH}$ = 6.0 Hz) and 4.90 ppm ($^2J_{PH}$ = 6.0 Hz), respectively, for the vinylic protons of **3c** and **3d**. Of the two isomeric structures C and D (Chart I) it might be expected that the relatively small J_{PH} coupling constant of 6.0 Hz would be inconsistent with structure D, where the coupled vinylic hydrogen is three bonds removed. However, for the structurally related phosphinidene/phenylacetylene coupled complex $Fe_2(CO)_6[^tBuPC(Ph)=CH]$, which also possesses a four-membered M–C–C–P metallacyclobutene ring,[27] a $^3J_{PH}$ value of 38 Hz has been observed and small $^2J_{PH}$ couplings of 10–20 Hz have been measured for vinylic protons in

(25) Garrou, P. E. *Chem. Rev.* **1981**, *81*, 229.
(26) Hietkamp, S.; Stuftens, D. J.; Vrieze, K. *J. Organomet. Chem.* **1977**, *139*, 189.
(27) Hang, H.; Zsolnai, L.; Huttner, G. *Chem. Ber.* **1985**, *118*, 4426.

alkenylphosphine complexes.[5,28] We tentatively favor structure C for **3c** and **3d**.

X-ray Structure of 3a. An ORTEP plot for **3a** is illustrated in Figure 3. The molecule is related to **2a** by the elimination of the ketonic carbonyl and coupling of an olefinic carbon atom to phosphorus. As a result of the change in metallacyclic ring size from the five-membered $\overline{RuC_3P}$ in **2a** to the four-membered $\overline{RuC_2P}$ in **3a** there is a major decrease in all of the intracyclic angles. Thus, Ru–P–C decreases from 103.8 (1)° (Ru–P–C(7) in **2a**) to 85.1 (1)° (Ru–P–C(8) in **3a**) and the angles subtended at the olefinic carbon atoms change from 120.5 (1)° (Ru–C(8)–C(9)) and 120.6 (1)° (C(7)–C(9)–C(8)) in **2a** to 103.9 (1)° (Ru–C(7)–C(8)) and 100.7 (1)° (C(7)–C(8)–P) in **3a**.

In terms of the interaction of the $PC(O)C(R^1)=C(R^2)$- and $PC(R^1)=C(R^2)$- systems of **2a** and **3a**, respectively, with the metals, the principal changes appear to be (i) a greater distortion in the pseudooctahedral geometry at ruthenium, (ii) a shortening of the Ru–Co bond length (2.6577 (4) Å in **2a**, 2.6479 (7) Å in **3a**) and an elongation of the Ru–P bond lengths (2.3335 (8) Å in **2a**, 2.3595 (1) Å in **3a**), (iii) a shortening and strengthening of the Ru–C and Co–C bonds to the metallacycle in **3a** (Co–C(9) = 2.180 (3) Å in **2a**, Co–C(8) = 2.110 (4) Å in **3a**; Co–C(8) = 2.008 (3) Å in **2a**, Co–C(7) = 1.997 (4) Å in **3a**; Ru–C(8) = 2.152 (3) Å in **2a**, Ru–C(7) = 2.136 (4) Å in **3a**), and (iv) a weakening of the interaction between the ruthenium atom and the asymmetrically bridging carbonyl carbon atom (Ru–C(5) = 2.380 (4) Å in **2a**, Ru–C(6) = 2.523 (6) Å in **3a**).

The structure of **3a** bears a rather strong resemblance to that of the heterobinuclear molecule $(CO)_3Fe(\mu\text{-}\eta^3\text{-}Ph_2PC(Ph)=C(Ph))Ni(\eta^5\text{-}C_5H_5)$, originally described[12a] as the $\mu_2\text{-}\eta^2\text{-}(\pi\text{-alkyne})$ complex $(CO)_3Fe(\mu\text{-}Ph_2P)(PhC{\equiv}CPh)Ni(\eta^5\text{-}C_5H_5)$ but subsequently shown by X-ray analysis[12b] to be a product of acetylene insertion in the phosphido bridge. There are substantial similarities between the ring systems of **3a** and the latter FeNi heterobinuclear compound, as shown by the angles Ru–P–C(8) of 85.1 (1)° in **3a** and the corresponding Fe–P–C angle of 84.6 (3)° in $(CO)_3Fe(\mu\text{-}\eta^3\text{-}Ph_2PC(Ph)=C(Ph))Ni(\eta^5\text{-}C_5H_5)$, as well as the internal P–C and C–C distances (P–C(7) = 1.809 (5) Å in **3a** vs P–C = 1.80 (1) Å; C(7)–C(8) = 1.440 (6) Å in **3a** vs 1.45 (1) Å).

There is also an interesting comparison between **3a** and the binuclear iron complex synthesized by Huttner et al.[27] via the reaction of the phosphinidene-bridged intermediate $[Fe_2(CO)_6(\mu\text{-}PBu^t)]$ with PhC≡CPh. In this molecule, however, phosphinidene–acetylene coupling generates a bridging phosphido group rather than a phosphine; hence, the phosphorus atom remains bridging to both metals.

Other Reactions Relevant to the Transformations 1 → 2 → 3. Phosphine Substitution and Alkyne Exchange: Mechanistic Implications. Since the synthesis of compounds of type **2** involves the incorporation of CO from the precursor into the organic fragment, we examined the influence of the tertiary phosphine PPh_2Me on the reaction of **1** with PhC≡CPh. No reaction took place at ambient temperature, and at 60 °C only the products of carbonyl substitution $(PPh_2Me)_n(CO)_{4-n}Ru(\mu\text{-}PPh_2)Co(CO)_3$ (n = 1, 2), previously characterized,[8] were obtained. Thus, PPh_2Me inhibits the formation of **2** or derivatives thereof. Previous work has shown that a CO ligand can be displaced from the ruthenium atom of **1** by Me_3NO in THF[9b] or a strong base (DBU),[11a] providing a vacant (or a solvent-occupied) site for coordination of a Lewis base. In an effort to secure evidence for an intermediate ruthenium-coordinated π-alkyne complex en route to **2**, complex **1** was treated with Me_3NO followed by 1 equiv of PhC≡CPh. No π-acetylene intermediate was detectable by infrared spectroscopy, and conversion to **2** did not occur. This result suggests that alkyne substitution at ruthenium is unlikely to be a key step in the formation of **2** from **1**.

Scheme II

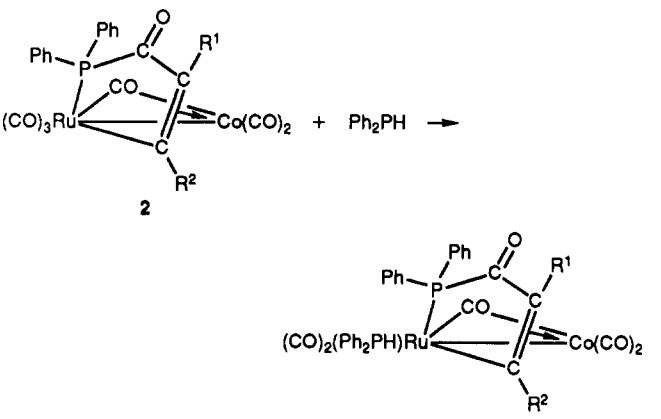

R^1, R^2 = Ph, Ph (**a**), H,Ph (**b**), H, $SiMe_3$, H (**c**)

In other binuclear complexes containing carbonylphosphine ligands related to those in **2**, reactions with an excess of alkyne lead to incorporation of a second alkyne.[14] Reaction of **2a** with ^{t}BuC≡CH at 50 °C leads, however, to alkyne exchange, affording 65% of the derivative **2d** and 25% of the precursor **2a** as well as traces of **3a** and **3d**:

$$\mathbf{2a} + {}^t\text{BuC}{\equiv}\text{CH} \rightarrow \mathbf{2d} + \text{PhC}{\equiv}\text{CPh}$$

This is a remarkable reaction considering that the PhC_2Ph fragment of **2a** is no longer present as an alkyne and is bound to both metals as well as the ketonic carbonyl group. Clearly a mechanism must exist for alkyne exchange that does not involve alkyne–alkyne coupling. The conversion of **2** to **3** involves the loss of a ketonic CO group and P–C(alkyne) coupling. Creation of a vacant metal site does not seem to be a prerequisite for this decarbonylation sequence, since the reaction of **2a** with Me_3NO in THF leads only to decomposition, with no **3a** being detected. Reaction of complexes **2a**, **2c**, and **2e** with Ph_2PH in THF did lead to the new products **4a**, **4c**, and **4e**, but these were carbonyl monosubstitution products of **2**[7] rather than derivatives of the decarbonylated species **3** (Scheme II). The ^{1}H and the $^{31}P\{^1H\}$ NMR spectra confirmed the retention of the organic ligand fragment of **2** and showed that **4a**, **4c**, and **4e** exist in solution as a mixture of isomers with trans and cis stereochemistries relative to the diphenylphosphino group of the carbonylphosphine, the trans isomers predominating. Thus, for **4a**, the $^{31}P\{^1H\}$ NMR spectrum exhibited two doublets at 42.8 and 23.9 ppm with a large J_{PP} value of 256.3 Hz, consistent with a mutual trans disposition of PPh_2 and Ph_2PH ligands. The higher field signal was identified as that of the secondary phosphine by virtue of a large $^1J_{PH}$ coupling of 366 Hz. In the cis isomers of **4** (e.g. **4e**, δ 48.4 (d, PPh_2), δ 26.8 (d, PPh_2H), $^2J_{PP}$ = 24.9 Hz) much smaller phosphorus–phosphorus couplings were observed, as expected from previous work.[8,9,11]

The above results shed relatively little light on the detailed mechanisms of the reactions **1** → **2** and **2** → **3**. Attempts to detect intermediates and gain spectroscopic insights by NMR techniques were compromised by the fact that the reactions do not proceed at low temperatures and

(28) Robert, P.; LeBozec, H.; Dixneuf, P. H.; Hartstock, F.; Taylor, N. J.; Carty, A. J. *Organometallics* **1982**, *1*, 1148.

Scheme III

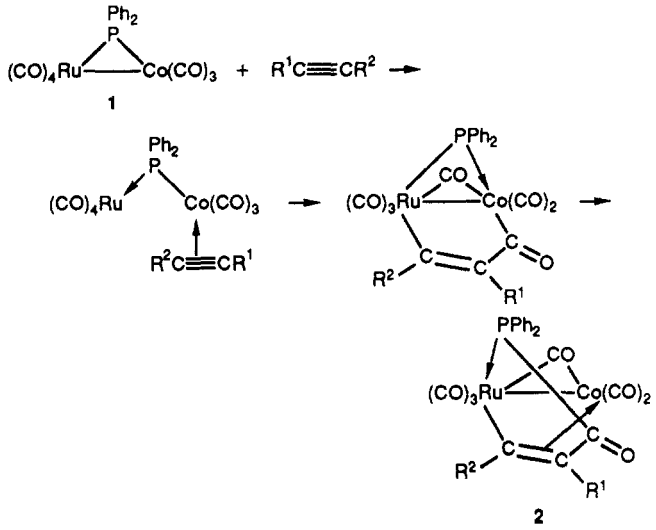

that, at higher temperatures, broadening due to quadrupolar coupling to ^{59}Co is a complicating factor. For a heterobinuclear phosphido-bridged molecule such as 1 initial reaction with a Lewis base might occur via associative or dissociative pathways, with the possibility of Ru–Co bond cleavage and/or phosphido bridge opening being involved in the former. There is good evidence that closely related molecules such as 34-electron $FeCo(CO)_7(\mu\text{-}AsR_2)$[29] and $FeCo(CO)_7(\mu\text{-}PPh_2)$[30] react associatively with phosphines and phosphites via Fe–Co bond cleavage to give 36-electron intermediates in which the added nucleophile is bound to the Co atom. Metal–metal bond closure yields the *kinetic* cobalt substitution products $(CO)_4Fe(\mu\text{-}MR_2)Co(CO)_2L$, which however isomerize to the *thermodynamically* stable iron substitution complexes $L(CO)_3Fe(\mu\text{-}MR_2)Co(CO)_3$.[29,30] For reactions of 1 with phosphines and phosphites, only the thermodynamic products of substitution at ruthenium $(CO)_{4-n}L_nRu(\mu\text{-}PPh_2)CoCO)_3$ (n = 1, 2)[8b] or the trisubstituted complexes $(CO)_2L_2Ru(\mu\text{-}PPh_2)Co(CO)_2L$[9c] have been identified. Given these facts and the experimental observations above, an attractive mechanism for the reaction of 1 with $R^1C{\equiv}CR^2$ would involve associative coordination of the acetylene at cobalt with Ru–Co bond cleavage, insertion of CO from cobalt into a Co–C(alkyne) bond coupled with Ru–C(alkyne) bond formation, migration of a carbonyl bridge from ruthenium to cobalt, and coupling of cis PPh_2 and acyl ligands at cobalt (Scheme III).

Comments on Alkyne Insertions into Phosphido Bridges. Since the first examples of products derived from insertion of acetylenes into PR_2 bridges were structurally characterized,[12-14] there have been a number of reports documenting similar reactivity in bi- and polynuclear complexes. The compounds described in the present paper represent some of the simplest examples of phosphido–acetylene coupling. Thus, the 1 to 3 transformation results in the conversion of the three-electron-donor $\mu\text{-}PPh_2$ group to a five-electron phosphinoalkenyl ligand. The CO insertion products 2 are (phosphinocarbonyl)-alkenyl ligands and also five-electron donors. Not surprisingly, more complex ligand systems may be produced when further alkyne insertions or coupling to other unsaturated ligands can occur, as illustrated by the generation of $R_2PC(R')=C(R'')C=C(R''')C(O)$- and $R_2PC(O)C(R')-C=C(R'')CR'''$- from $Fe_2(CO)_6(\mu\text{-}PPh_2)(\mu\text{-}\eta^2\text{-}C{\equiv}CR''')$.[14] Among other closely related examples of unsaturated ligand–phosphido bridge coupling reported are the following: the synthesis of $[Cp^*_2Co_2(\mu\text{-}PMe_2)(\mu\text{-}Me_2PC(CO_2Me)=CHC(O)OMe)]BF_4$ from $[Cp^*_2Co_2(\mu\text{-}PMe_2)_2(\mu\text{-}H)]BF_4$ and $C_2(COOMe)_2$,[15] the preparation of phosphinoalkene and phosphinobutadiene complexes from phosphido (alkenyl) bridged dimanganese compounds,[5] (phosphinoalkenyl)-dimolybdenum compounds from phosphido μ-alkyne species,[31] the generation of an unusual $Ru_3(CO)_{10}[\mu\text{-}C_6H_4(PhPCH_2PPh)]$ cluster from an ortho-metalated phosphido phosphine via intramolecular P–C coupling,[32] and the synthesis of Ru_3 and Ru_4 phosphinoalkenyl clusters from phosphido-bridged complexes and acetylenes.[33] These $\mu\text{-}PR_2$–unsaturated ligand coupling reactions are by no means unique in phosphido chemistry. Thus, insertion of acetylenes into M–P bonds of $M_n(\mu_3\text{-}PR)$ clusters affords an entry into the interesting class of ternary clusters with metals, phosphorus, and carbon in the framework.[16-18] The electronic structures and skeletal rearrangement of these molecules have been extensively investigated by Huttner and co-workers.[34]

It is now clear that while the $\mu\text{-}PR_2$ bridge can under certain conditions behave essentially as an inert spectator ligand, intra- or intermolecular coupling reactions should be expected in the presence of reactive unsaturated hydrocarbyls, especially under thermal or photochemical activation. Indeed, with evidence of phosphido bridge mobility and transferability between metal centers[35] many other interesting coupling reactions can be expected.

Acknowledgment. We are grateful to the NSERC (Canada) and the CNRS and MENJS (France) for financial support of this research.

Supplementary Material Available: For each molecule, tables of anisotropic thermal parameters, hydrogen atomic positions and isotropic thermal parameters, and the remaining bond lengths and angles (respectively Tables S1–S3 for **2a**, S4–S6 for **2e**, and S7–S9 for **3a**) (9 pages); tables of structure factors (Table S10 for **2a**, Table S11 for **2e**, and Table S12 for **3a**) (54 pages). Ordering information is given on any current masthead page.

(29) Langenbach, H. J.; Vahrenkamp, H. *Chem. Ber.* **1979**, *112*, 3391 and references therein.
(30) Baker, R. T.; Calabrese, J. C.; Krusic, P. J.; Therien, M. J.; Trogler, W. C. *J. Am. Chem. Soc.* **1988**, *110*, 8392.
(31) Conole, G.; Hill, K. A.; McPartlin, M.; Mays, M. J.; Morris, M. J. *J. Chem. Soc., Chem. Commun.* **1989**, 688.
(32) Lugan, N.; Bonnet, J. J.; Ibers, J. A. *Organometallics* **1988**, *7*, 1538.
(33) Van Gastel, F.; Sappa, E.; Tiripicchio, A.; Carty, A. J. *J. Organomet. Chem.*, in press.
(34) (a) Knoll, L.; Huttner, G.; Zsolnai, L.; Orama, O. *Angew. Chem., int. Ed. Engl.* **1986**, *25*, 119. (b) Huttner, G.; Knoll, K.; Fassler, T.; Berke, H. *J. Organomet. Chem.* **1988**, *340*, 223.
(35) Davies, S. J.; Howard, J. A. K.; Pilotti, M. U.; Stone, F. G. A. *J. Chem. Soc., Chem. Commun.* **1989**, 190.